Journal of Catalysis 286 (2012) 165–171

Contents lists available at SciVerse ScienceDirect

Journal of Catalysis

journal homepage: www.elsevier.com/locate/jcat

Combined in situ QXAFS and FTIR analysis of a Ni phosphide catalyst under hydrodesulfurization conditions

Kyoko K. Bando [a,*], Takahiro Wada [b], Takeshi Miyamoto [b], Kotaro Miyazaki [b], Satoru Takakusagi [b], Yuichiro Koike [c], Yasuhiro Inada [d], Masaharu Nomura [c], Aritomo Yamaguchi [e], Travis Gott [f], S. Ted Oyama [f,g], Kiyotaka Asakura [b,*]

[a] Nanosystem Research Institute, National Institute of Advanced Industrial Science and Technology, 1-1-1 Higashi, Tsukuba, Ibaraki 305-8565, Japan
[b] Catalysis Research Center, Hokkaido University, Kita-ku N21W10, Sapporo, Hokkaido 001-0021, Japan
[c] Photon Factory, Institute of Materials Structure Science, High Energy Accelerator Research Organization, Oho 1-1, Tsukuba, Ibaraki 305-0801, Japan
[d] College of Life Science, Ritsumeikan University, 1-1-1 Noji Higashi, Kusatsu, Shiga 525-8577, Japan
[e] Research Center for Compact Chemical System, National Institute of Advanced Industrial Science and Technology, AIST Tohoku, 4-2-1 Nigatake, Miyagino-ku, Sendai, Miyagi 983-8551, Japan
[f] Environmental Catalysis and Materials Laboratory, Department of Chemical Engineering and Chemistry, Virginia Polytechnic Institute and State University, Blacksburg, VA 24061-0211, USA
[g] Department of Chemical Systems Engineering, The University of Tokyo, 7-3-1 Hongo, Bunkyo-ku, Tokyo 113-8656, Japan

ARTICLE INFO

Article history:
Received 20 July 2011
Revised 21 September 2011
Accepted 26 October 2011
Available online 2 December 2011

Keywords:
Ni_2P
HDS
QXAFS
FTIR
Thiophene
MCM-41
In situ
Simultaneous time-resolved study

ABSTRACT

Supported Ni_2P catalysts are active for hydrodesulfurization (HDS) of petroleum feedstocks and have attracted considerable attention. In order to find out the structure of the active catalyst and to obtain insight into the reaction mechanism of thiophene HDS over Ni_2P/MCM-41, we conducted a simultaneous time-resolved (STR) study with in situ X-ray absorption fine structure (XAFS) spectroscopy and Fourier transform infrared (FTIR) spectroscopy together with time-resolved product analysis. At 513 K, adsorbed tetrahydrothiophene (THT) was observed by FTIR, following the formation of a nickel phosphosulfide phase (NiPS). Detection of the HDS products coincided with the THT formation. All these experimental data indicated that NiPS worked as the active phase and identified THT as a reaction intermediate for the HDS reaction. The STR study proved to be a powerful tool for the precise study of reaction intermediates and the catalytic reaction path.

1. Introduction

Since the first report that showed the potential of phosphide compounds as hydrodesulfurization (HDS) catalysts [1], metal phosphide materials have attracted much attention and a lot of effort has been expended to develop catalysts whose activities surpass those of current industrial catalysts [2,3]. Molybdenum and tungsten are the major components of commercial HDS catalysts, and they are present in sulfide form [4]. Phosphides of Mo and W were also applied to the HDS reaction, and they were found to have substantial activities, comparable to the sulfide forms based on turnover frequencies [5,6]. Further investigations revealed that nickel phosphide had the highest performance in terms of turnover frequency and could be considered a promising candidate as a next-generation HDS catalyst [2,7]. Detailed characterization of the active Ni phosphide revealed that the active phase had a Ni_2P composition [8–10] and that this phase had high performance due to its high resistance to sulfur. Analysis by X-ray diffraction and extended X-ray absorption fine structure (EXAFS) showed that the bulk Ni_2P structure was retained after HDS reaction of real oil [11]. Another feature of Ni_2P is that the smaller nanoparticles possess higher turnover frequency (TOF) [12]. When HDS of 4,6-dimethyldibenzothiophene (4,6-DMDBT) was applied to Ni_2P/SiO_2 with different Ni_2P particle sizes, the TOF of small particles (3.8 nm) was larger than that of large particles (10.1 nm), and in addition, smaller particles favored HDS through the hydrogenation route [12,13]. Moreover, in situ X-ray absorption fine structure (XAFS) under reaction conditions showed the presence of sulfur on Ni_2P after the HDS reaction, which seemed to work as a promoter rather than a poison

* Corresponding authors. Fax: +81 29 861 6236 (K.K. Bando), fax: +81 11 706 9113 (K. Asakura).
E-mail addresses: kk.bando@aist.go.jp (K.K. Bando), askr@cat.hokudai.ac.jp (K. Asakura).

0021-9517/$ - see front matter © 2011 Elsevier Inc. All rights reserved.
doi:10.1016/j.jcat.2011.10.025

[12,14,15]. Although overall kinetic studies have been conducted [16], details about each elementary step and the active structures are still under investigation [17].

In this work, simultaneous time-resolved (STR) analysis of Ni_2P/MCM-41 under thiophene HDS conditions was carried out using in situ quick X-ray absorption fine structure (QXAFS) analysis, in situ Fourier transform infrared (FTIR) spectroscopy and mass spectroscopy. We have already applied in situ QXAFS and in situ FTIR to this catalyst system separately [17]. In that study, EXAFS showed the formation of a NiPS species and FTIR showed that tetrahydrothiophene (THT) was an adsorbed species present during reaction. Even though the experimental parameters were set as close as possible to the same conditions, it was difficult in that experiment to obtain an exact time correlation between the two sets of spectra with sufficient time resolution to allow conclusions about the reaction path. Thus, we could not conclusively confirm whether THT was the intermediate produced by hydrogenation of thiophene or THT was just a spectator. In this study, a new in situ system was developed, which could measure in situ QXAFS and FTIR simultaneously at the same position on the same sample [18]. The combined use of in situ XAFS with other in situ techniques is a very useful characterization tool of catalysts. Initial work can be found in the combination of XAFS and XRD analysis [19–21]. Recently, pioneering work has been reported in simultaneous or synchronous analyses of catalysts by using combined in situ techniques such as XAFS-UV or XAFS-IR [22–27]. These outstanding studies could reveal the effect of X-ray irradiation and adsorption-induced morphology changes in the catalyst. The combination of XAFS and IR is most promising because XAFS provides the structure of the catalyst and its change, while IR provides direct information on adsorbates. A setup employing diffuse reflectance infrared spectroscopy (DRIFT) and mass spectrometry (MS) combined with XAFS was path-breaking but required a long sample cell length, and the XAFS measurements were limited to elements with high K-edge energy such as Rh and Pd [23,25,24]. But recently, measurement of Ni K-edge was performed with an improved XAFS-DRIFT system [27]. The present work builds on these precedent works by combining, for the first time, transmission FTIR with XAFS using a portable FTIR spectrometer equipped with optical fibers for light transmission, which realizes a compact design [18]. An attractive feature is that both the FTIR and XAFS techniques allowed the use of nearly the same optimal sample amount of Ni_2P/MCM-41. The system enabled the measurement of simultaneous time-resolved (STR) QXAFS, FTIR and online gas analysis. This STR method can be used to determine more exactly the sequence of the structural changes in the catalyst and the adsorbate, while permitting the monitoring of the formation of the product, which gives direct information about the reaction path, active site structure and intermediate species.

2. Experimental

2.1. Sample preparation

This work used as the support a silicious MCM-41 synthesized following a procedure reported in the literature [28]. Preparation of the supported Ni_2P was conducted by impregnation of nickel and phosphorous precursors followed by calcination and temperature-programmed reduction (TPR), as described elsewhere [17]. The loading of Ni was 1.15 mmol Ni $g^{-1}_{support}$ (12.2 wt.% Ni_2P/support). An excess amount of phosphorus (Ni/P = 1/2) was used because some of the phosphorus formed PH_3 in the course of the reduction [17]. After Ni_2P was formed on the catalyst by TPR, the sample was cooled to room temperature in flowing He and was passivated in a flow of 0.5% O_2/He for 4 h to prevent uncontrolled oxidation of the freshly produced phosphide.

2.2. XAFS analysis

Preliminary in situ QXAFS measurements were carried out at beam line NW10A of Photon Factory Advanced Ring (PF-AR) attached to a 6.5 GeV storage ring. The STR data discussed in this paper were collected at beam line 9C (BL9C) of Photon Factory (PF) with a ring operated at 2.5 GeV and 430 mA. Both of the beam lines belong to Institute of Materials Structure Science (IMSS), High Energy Accelerator Research Organization (KEK) in Japan. A bent-cylindrical mirror focused the X-ray on the sample and a Si(1 1 1) double crystal monochromator continuously rotated from 14.164° to 12.836° to monochromatized the light in the energy range from 8080 to 8900 eV. A typical QXAFS scan of the Ni K-edge had 2147 steps and took 10 s. The XAFS spectra were observed in transmittance mode, and the intensity of the incident X-ray beam (I_0) and transmitted beam (I) was measured by ionization chambers filled with 100% N_2 and 25% Ar in N_2, respectively. An as-observed QXAFS spectrum was processed with smoothing and interpolation to reduce the number of data points to 770, which makes the spectrum available for XAFS analysis programs. The obtained spectrum was regarded as a raw spectrum and analyzed by the software program REX2000 (Rigaku Co.). Curve-fitting analysis was carried out with parameters obtained with FEFF8 (Univ. of Washington).

2.3. Combined QXAFS and FTIR analysis

The simultaneous measurement of QXAFS and FTIR utilized an in situ cell in the shape of a cross (Fig. 1) [18]. The sample in the form of a pressed wafer was set in the center of the cell. The X-ray and IR beams went through the cell in two perpendicular directions and met each other orthogonally at the center of the cell, where the sample was positioned at 45° to both beams. Simultaneously with QXAFS observation described in the Section 2.1, the FTIR spectra were collected every 60 s by a JASCO VIR-9500. The incident IR beam was carried to the reactor with an optical fiber (ZnSe), and the transmitted IR beam was detected by an MCT detector, which was placed on the same stage as the cell. Consequently, alignment of the IR and XAFS optical axes could be performed easily. Polyimide films (125 μm in thickness) and KBr disks (3 mm in thickness) were used as the X-ray and FTIR window materials, respectively. With this setup, this cell can be safely operated up to 0.3 MPa, but since the body of the cell is made of stainless steel, it can be used at higher pressure, selecting an appropriate material for windows.

The reactant gas was introduced to the cell from ports near the four windows, and the product gas was let out from the center of

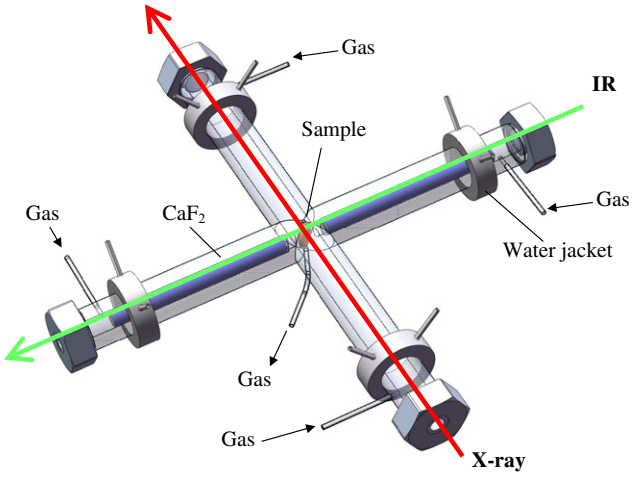

Fig. 1. Diagram of an in situ cell for simultaneous measurement of XAFS and IR.

the cell, so the windows were not subject to undesirable heating. Windows can be kept at ambient temperature, when the sample is heated up at 803 K. In addition to that, CaF_2 crystal rods were placed in the IR optical path to minimize the dead volume (38 cm^3) and suppress absorption of the IR radiation by gas-phase species. This gas flow design also reduced dead volume and minimized the stagnation regions of the reactant gas and enabled quick gas exchange to make the cell suitable for kinetic studies.

2.4. In situ experiments

An amount of 35 mg of catalyst pressed into a wafer of 15 mm in diameter and about 0.4 mm in thickness was set at the center of the in situ cell. Activation of the catalyst was carried out under H_2 flow at a rate of 50 or 100 cm^3 (NTP)/min. The temperature was raised from room temperature to the final temperature (723 K or 803 K) at a rate of 5 K/min and kept there for 2 h. After activation, the catalyst was cooled to the reaction temperature under H_2 flow, after which the gas was switched to a reactant mixture composed of thiophene (0.1 vol.%), He (1.8 vol.%) and H_2 (98 vol.%) at a total flow rate of 102 cm^3 (NTP)/min under atmospheric pressure. The reaction products were monitored by an online quadrupole mass spectrometer (QMS, Hyden Analytical HAL301). In order to remove the unreacted thiophene, H_2S and flammable gases, the exhaust gas was treated with an HDS reactor with a CoMoS catalyst, H_2S absorber (composed of $NaOH_{aq}$ solution followed by a ZnO bed) and a burner, respectively. As a result, only water and CO_2 were emitted from the reaction system.

3. Results and discussion

Since the finding that Ni_2P is an efficient catalyst for HDS, considerable effort has been expended in improving the catalytic activity and in investigating the structure of the active sites and the reaction mechanism [2]. One of the main reasons for the high HDS performance of Ni_2P was thought to be attributed to its high tolerance to sulfur. Even after the HDS reaction with real and model oils, it still retains the Ni_2P bulk structure [11,29]. However, previous studies also suggested the formation of a surface phosphosulfide (NiPS) phase during reaction [8,12,34,30]. Since the formation of Ni–S occurred only on the Ni_2P surface, the number of the Ni–S bonds was small compared to the Ni–P bonds. As will be shown, in situ XAFS is particularly suited to detect the small amount of Ni–S and to follow changes occurring on the surface of Ni_2P [17,34], because it allows a direct comparison of samples before and during reaction, without disturbing the sample. These measurements, as well as simultaneous in situ FTIR measurements, are the subject of this paper.

3.1. Activation process

Figs. 2 and 3 show the Ni K-edge XANES and Fourier transform (FT, the phase shift is not corrected) of EXAFS ($k^3\chi(k)$) spectra of Ni_2P/MCM-41 before and after activation by reduction in hydrogen (the k range Fourier transformation was 3–10 $(0.1\ nm)^{-1}$ and 3–12 $(0.1\ nm)^{-1}$ for Fig. 3a and b, respectively). Table 1 shows the results of curve-fitting analysis of the peaks in Fig. 3. The curve-fitting analysis was conducted for EXAFS oscillations ($k^3\chi(k)$) in the k space, which were obtained by back Fourier transform of Fourier filtered FT spectra (0.107–0.344 and 0.089–0.301 nm for Fig. 3a and b, respectively). Before the activation, there were two peaks in the FT (Fig. 3a), and they were assigned to Ni–O bonds (N (coordination number) = 4.2 ± 0.7, R (distance) = 0.203 ± 0.002 nm) and Ni–Ni bonds (N = 5.1 ± 1.5, R = 0.309 ± 0.003 nm). Judging from the distances, the species before the activation had a similar structure to that of $Ni(OH)_2$ [31]. After 2 h of reduction at 723 K (Fig. 2, solid line), the XANES spectrum changed to one very similar to that of Ni_2P [32]. After the activation, there was one broad peak in the FT as shown in Fig. 3b. Curve-fitting analysis of this peak gives contributions of Ni–P (N = 2.9 ± 0.6, R = 0.222 ± 0.002 nm) and Ni–Ni (N = 3.4 ± 0.8, R = 0.256 ± 0.002 nm) (Table 1). The distances corresponded to those of Ni_2P [8]. The particle size was estimated at 1 nm, which, as expected, was close to that of Ni_2P on another mesoporous system, Ni_2P on KUSY [31].

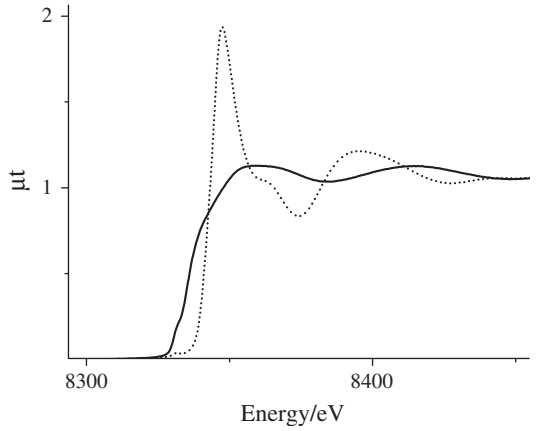

Fig. 2. Ni K-edge XANES spectra of Ni_2P/MCM-41 before (dotted line) and after activation at 723 K under H_2 for 2 h (solid line).

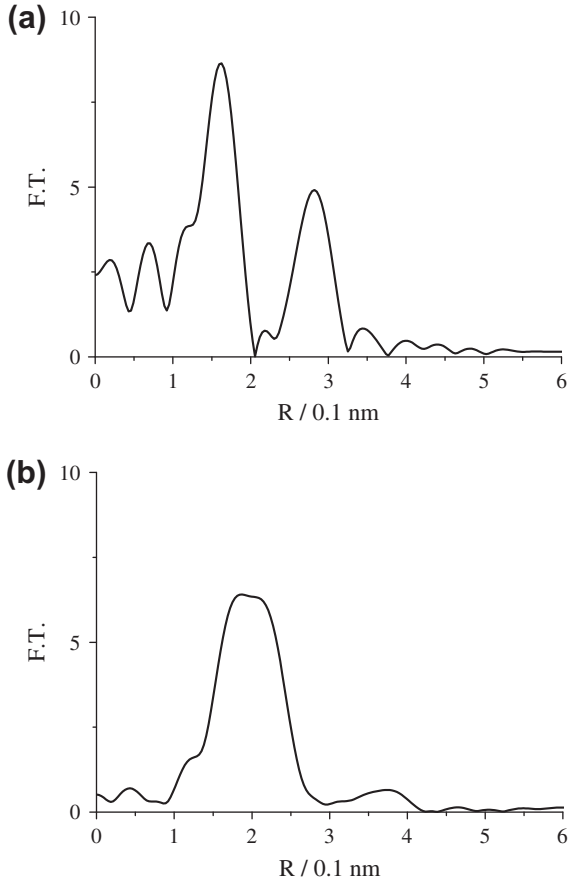

Fig. 3. Fourier transform of Ni K-edge EXAFS ($k^3\chi(k)$) for Ni_2P/MCM-41, (a) before activation and (b) after activation at 723 K under H_2 for 2 h. The phase shift is not corrected.

Table 1
Curve-fitting results for Ni_2P/MCM-41.

Condition	Scattering	N	R (nm)	ΔE (eV)	σ (nm)	R factor (%)
Before TPR	Ni–O	4.2 ± 0.7	0.203 ± 0.002	−8 ± 1	0.005 ± 0.001	0.15
	Ni–Ni	5.1 ± 1.5	0.309 ± 0.003	−0.3 ± 2	0.011 ± 0.002	
After TPR	Ni–P	2.9 ± 0.6	0.222 ± 0.002	−0.9 ± 1	0.0094 ± 0.001	0.04
	Ni–Ni	3.4 ± 0.8	0.256 ± 0.002	−0.3 ± 3	0.010 ± 0.001	
Difference between before and during HDS	Ni–S	0.3 ± 0.2	0.233 ± 0.005	6 ± 5	0.010 ± 0.004	2.3

3.2. Steady-state HDS

Fig. 4a shows Ni K-edge EXAFS oscillations observed for activated Ni_2P/MCM-41 before the HDS reaction ($k^3\chi_1(k)$, dotted line) and under HDS reaction conditions for 2 h ($k^3\chi_2(k)$, solid line) at 573 K. Each spectrum was produced from a sum of 30 raw spectra observed continuously under the same conditions. There was no discernible change between the EXAFS spectra before and during the reaction, like in the case of other Ni_2P catalysts [32,33]. However, the use of in situ XAFS, where the sample spot location and conditions can be reproduced exactly, allows a difference spectrum to be taken between the spectra of the reduced sample before reaction and the working catalyst at reaction conditions. This in essence subtracts the contribution of the bulk. The difference spectrum of these two ($k(\chi_2(k) - \chi_1(k))$) reveals very clearly a regular oscillation, which can be ascribed to the formation of a new bond (Fig. 4b). Curve-fitting analysis of this spectrum (Table 1, the k range for Fourier transform was 3–10 $(0.1\ nm)^{-1}$, the Fourier filter range was 0.10–0.27 nm and the fitting was conducted in the k space.) indicated that it is due to a Ni–S bond ($N = 0.3 \pm 0.2$, $R = 0.233 \pm 0.005$ nm) since the bond distance corresponded to those in known sulfides (0.225–0.240 nm) and not phosphides (0.218–0.231 nm). Similar results were already obtained in the case of a model oil HDS over Ni_2P/SiO_2 [34]. It is confirmed here that a small number of Ni–S bonds are present under thiophene HDS conditions, and what remains to be determined is the exact location and function of the sulfur.

Fig. 5 shows the corresponding Ni K-edge XANES of Ni_2P before and during the HDS reaction at 573 K. Like in the case of the EXAFS oscillations in Fig. 4, the difference in the XANES spectra before and during the reaction was so small that no change was found in the spectra drawn on a regular scale (Fig. 5a). However, when the pre-edge part of XANES of Fig. 5a was magnified and closely examined, it is found that there was a very small change between the two spectra at 8333.3 eV (Fig. 5b), with a shoulder feature at

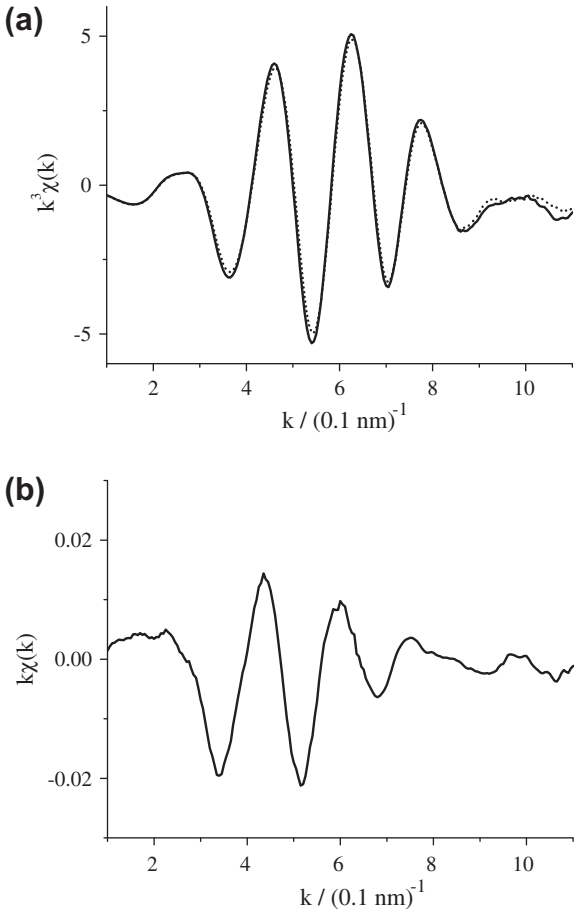

Fig. 4. Ni K-edge EXAFS oscillations for Ni_2P/MCM-41, (a) after activation at 573 K under H_2 (dotted line) and during thiophene HDS (solid line) and (b) difference spectrum.

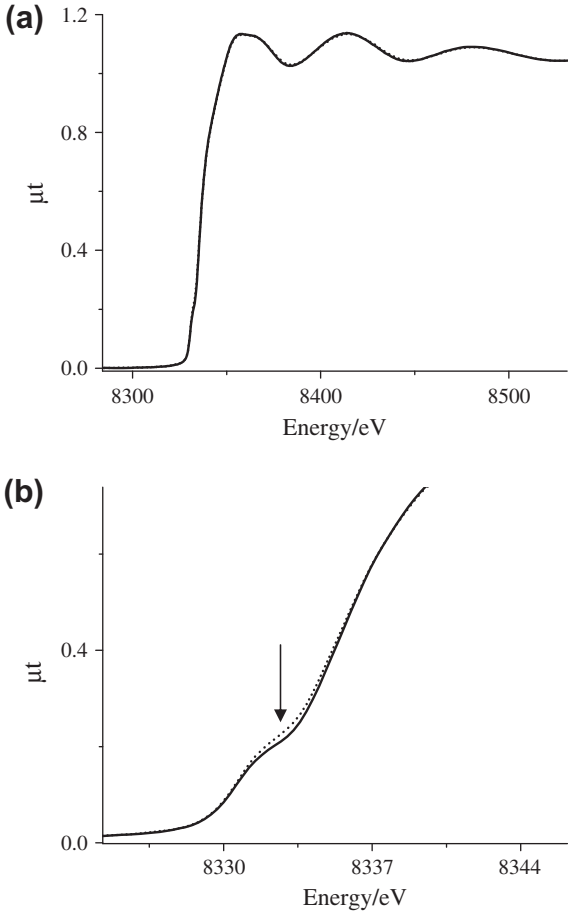

Fig. 5. Ni K-edge XANES spectra for Ni_2P/MCM-41, (a) after activation at 573 K under H_2 (dotted line) and during thiophene HDS (solid line) and (b) magnification of the pre-edge part of (a).

8333.3 eV decreasing slightly during reaction as marked by the arrow. Although the change was small, it was reproducible and corresponded well to the formation of Ni–S bonds detected by EXAFS as discussed above. The decrease in the XANES signal at 8333.3 eV is, therefore, assigned to the formation of Ni–S bonds in the Ni_2P catalyst.

There are three possibilities regarding the origin of the newly evolved Ni–S bond. First, it could be due to a bond between surface Ni and S of adsorbed thiophene or a derivative of thiophene (Case1). Second, it could be due to a bond between surface Ni and adsorbed atomic S, playing the role of a poison or less active species like nickel sulfide (NiS) (Case2). Finally, it could be associated with a sulfur atom in an active site or acting as a promoter like in the nickel phosphosulfide (NiPS) phase that has been postulated in previous studies [8,12,34] (Case3). In order to clarify the role and the property of Ni–S, further investigations were conducted.

3.3. XANES change during HDS

Fig. 6 shows the change in XANES intensity at 8333.3 eV during the initial 100 min of reaction at 573 K, 513 K and 453 K. Immediately after the reaction started, a rapid drop in XANES was observed at 573 K and 513 K, whereas a relatively gradual decrease was observed at 453 K. The Ni–S amount under steady state (after 100 min) estimated from the decrease in XANES was larger at higher reaction temperatures. The reaction products were analyzed simultaneously by the online QMS. The ratio of activity at steady-state conditions estimated from the H_2S signal ($m/z = 34$) was 17:1.4:0.3 for 573 K, 513 K and 453 K. The product analysis showed that the activity increased with reaction temperature. In our previous work, catalytic tests under the same conditions with an online GC were conducted. At all reaction temperatures, the selectivity for HDS products (butane and butenes) was 100%. The activities expressed in TOF are 0.0082, 0.0071 and 0.0058 s^{-1} for 573, 513 and 453 K, respectively [17], which gave the same trend in activity as the present study, that is, the activity increased with reaction temperature. The catalyst at higher temperature possessed more Ni–S on Ni_2P, suggesting that Ni–S is not a poison of the catalyst, since the activity increased with it. In order to find out whether the Ni–S bond was involved in the active phase, catalysts with different Ni–S coverage were compared under HDS conditions at 453 K. A catalyst with a large amount of Ni–S was produced by HDS at 573 K prior to the reaction at 453 K. The catalyst treated under HDS conditions at 573 K was cooled to 453 K under He, and the catalytic performance at 453 K was measured. The result was compared with that of HDS at 453 K over a catalyst that was simply activated in H_2. The ratio of the amount of Ni–S estimated from XANES and the HDS activity estimated from the H_2S signal of QMS are summarized in Table 2. The results show that the catalytic activity increased proportionally to the amount of Ni–S. We conclude that the Ni–S species is directly involved in the reaction path, either incorporated in the active site (Case 3) or associated with the active species (Case 1).

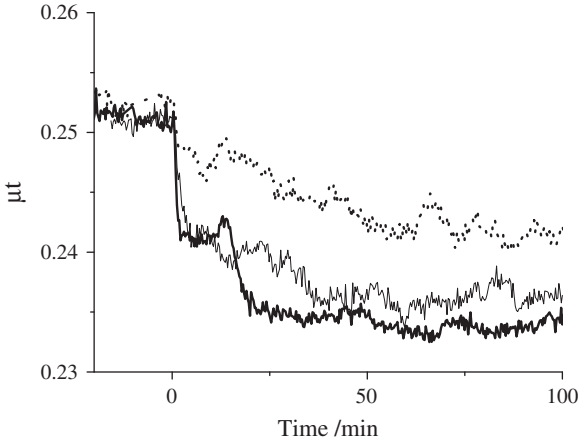

Fig. 6. Change in XANES at 8333.3 eV during HDS at 573 K (bold solid line), 513 K (fine solid line) and 453 K (dotted line).

Table 2
Correlation between the amount of Ni–S and the thiophene HDS activity at 453 K over Ni_2P/MCM-41.

	Pretreatment	
	Activation at 803 K	Activation at 803 K, followed by HDS at 573 K
$\frac{\text{Amount of Ni–S}}{\text{Amount of Ni–S treated at 573 K}}$ [a]	0.6	1
HDS activity/a.u.[b]	0.3	0.5

[a] Estimated with the decrease in XANES at 8333.3 eV.
[b] Estimated with production of H_2S (QMS, $m/z = 34$).

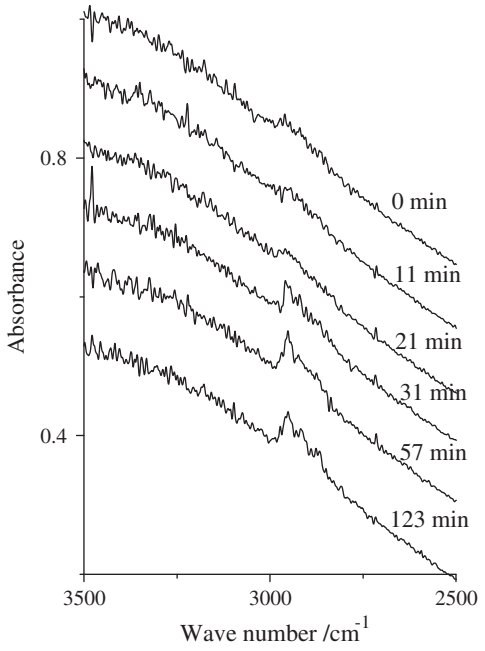

Fig. 7. Change in IR observed simultaneously with QXAFS (Fig. 6) during HDS at 513 K. The start time of each measurement is shown in the figure.

3.4. Simultaneous QXAFS and IR measurements

To distinguish between the two possibilities for the assignment of the Ni–S bond, that is, Case 1 or Case 3, measurements with FTIR were undertaken. The reasoning was that if the Ni–S found in XANES were due to adsorbed thiophene or tetrahydrothiophene (THT), a change in the XANES signal should result in a corresponding change in the IR spectra. Thiophene and THT adsorbed on Ni can be distinguished from the position of their C–H bands, which are quite distinctive since they originate from aromatic and aliphatic bonds. Thiophene has aromatic ν(CH) bands in the region from 3082 to 3134 cm^{-1}, while THT has aliphatic ν(CH) bands from 2876 to 2953 cm^{-1} [17]. Fig. 7 shows the FTIR bands for the adsorbed species during reaction at 513 K, and they clearly fall in the region for THT. The change in the FTIR peaks for THT was followed simultaneously with the XANES measurements. Very weak

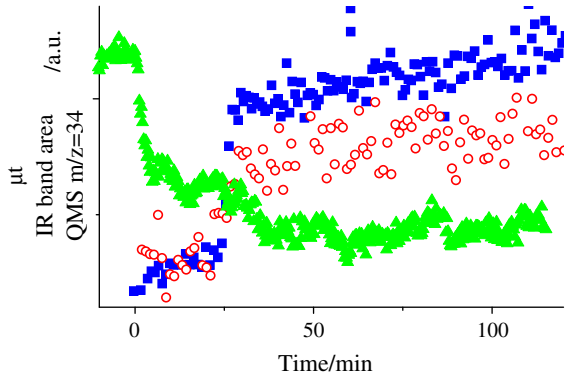

Fig. 8. Change in XANES at 8333.3 eV (triangles) compared with that of IR band in the aliphatic ν(CH) region (open circles) and the formation of H_2S detected by QMS (m/z = 34) (squares) during HDS at 513 K.

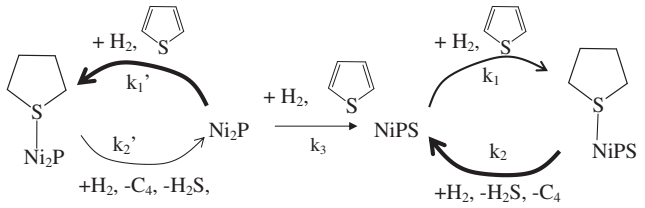

Scheme 1. Proposed reaction paths of thiophene HDS over the Ni_2P/MCM-41 catalyst.

peaks were observed in the aliphatic ν(CH) region at the beginning of the reaction, but they stayed at the same intensity for more than 10 min. After 20 min, the band suddenly began to increase and reached saturation at 57 min. Fig. 8 shows the change in the XANES signal at 8333.3 eV compared with the change in the IR band area in the aliphatic ν(CH) region during the reaction at 513 K. The change in H_2S production detected by QMS (m/z = 34) is also plotted in the same figure. As mentioned above, during the initial period of about 10 min when the XANES signal showed a rapid formation of Ni–S (the actual signal decreased), the IR band intensity stayed at a low level. But after 20 min passed when almost no more change was observed in the XANES, the IR band suddenly started to increase. These results show that the XANES changes are not due to the formation of a Ni–S bond between Ni and adsorbates such as THT or thiophene (Case 1). In addition to this, the H_2S production increased simultaneously with the IR ν(CH) band intensity. These results can be interpreted as follows: at the beginning of the reaction at 513 K, thiophene was hydrogenated and desulfurized to give H_2S, in the course of which the nickel phosphosulfide (NiPS) phase was formed. When the NiPS phase was saturated, the catalytic hydrogenation reaction channel of thiophene was activated to form intermediate THT species rapidly on the NiPS phase of the catalyst. These THT species were immediately converted into H_2S and desulfurized compounds. It is concluded that Case 3, that is, where the Ni–S bond is assigned to an active NiPS species, is the most appropriate among the three possibilities. Theoretical calculation of XANES based on the NiPS also supports this model [35], but detailed studies are now under way.

3.5. Overview

The Ni_2P catalyst has a high tolerance for sulfur compared to other Ni compounds. One of the reasons for this might be a strong interaction between Ni and P. In addition to that, under the HDS conditions employed in this work, formation of the NiPS phase is found to be favorable, and once the NiPS phase is generated and covers the Ni_2P particle, it facilitates activation of hydrogen molecules and promotes HDS, which prevents the corrosive attack of sulfur. Taking into account the coordination number obtained for Ni–S (=0.3) and the particle size of Ni_2P (=1 nm), about 40% of Ni atoms on the surface are involved in the NiPS phase. Since it is likely that the Ni atoms surrounding the NiPS sites are subjected to some influence from them, the effect of the NiPS phase spreads all over the Ni_2P surface. As a result, the NiPS surface phase works not only as an active site for the HDS reaction but also as a protecting layer on Ni_2P.

It was found that the HDS activity increased with the amount of Ni–S, and this was confirmed in the experiment where thiophene was pretreated at 573 K as shown in Table 2. The promoting effect

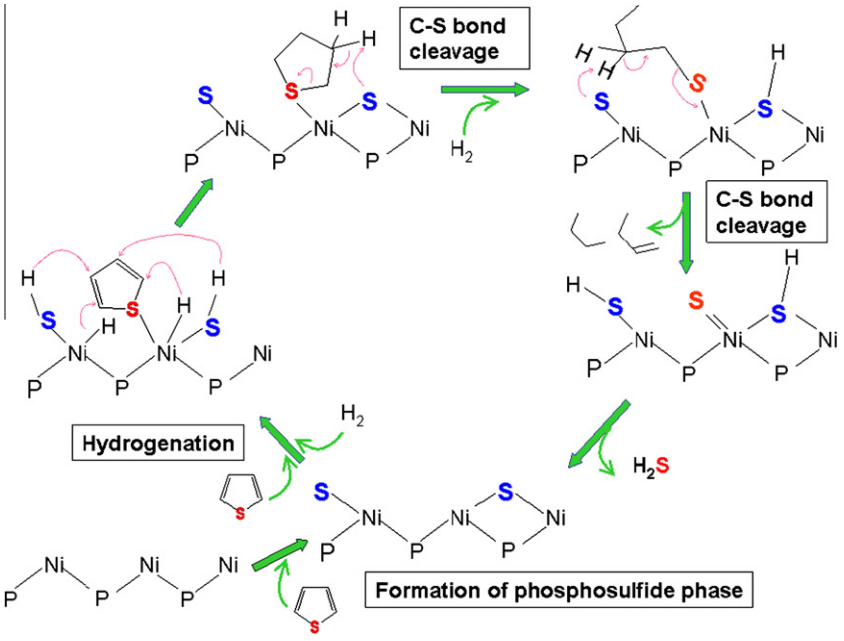

Scheme 2. Proposed mechanism of thiophene HDS reaction over nickel phosphosulfide.

by sulfur on Ni_2P was already reported in a study where a Ni_2P catalyst passivated with H_2S showed higher activity in the initial several hours of reaction than one that was pre-reduced [15].

In this work, the changes in the Ni–S bonds were followed by monitoring the XANES signal, while simultaneous time-resolved (STR) infrared measurements were carried out during the reaction at 513 K. This eliminates ambiguity in the interpretation of results obtained from other methods carried out at different times and in different units.

A direct correlation was found between the formation of Ni–S species observed by XANES, activity behavior and THT formation by the STR method. The XANES indicated that a considerable amount of Ni–S bond formation was necessary for high activity in H_2S formation. THT formation is clearly slow on the reduced Ni_2P surface without such surface modification. Once Ni–S formation reached a certain level, THT formation was suddenly observed.

The STR analysis gave another insight about the reaction mechanism. As shown in Fig. 8, at 513 K, the formation of THT (IR) and production of H_2S (QMS) started after the formation of NiPS species (XANES) was almost completed. Taking these facts into account, a reaction mechanism as shown in Scheme 1 is proposed. During the initial period, the HDS reaction proceeded slowly on Ni_2P, governed by rate constants k_1' and k_2', as shown in the left-hand cycle of Scheme 1. Small amounts of H_2S were detected in the reaction products, and a small signal due to adsorbed THT was observed by IR, the latter indicating that $k_1' > k_2'$. As the reaction proceeded, the surface became sulfided, producing NiPS competitively through rate constant k_3. As the surface NiPS phase formed, the HDS reaction rate accelerated, and the reaction switched to the right-hand cycle, governed by rate constants k_1 and k_2. Scheme 2 shows a detailed series of steps for the right-hand cycle in Scheme 1. It is speculated that sulfur in the NiPS phase during HDS of thiophene assists in hydrogen transfer. The sulfur in NiPS occupies one coordination site on a Ni atom, which promotes H_2 activation by providing adsorption sites for cleaved hydrogen. Although the scheme shows the possible transfer of four H atoms, this is a special case. It is quite likely that only a pair of H atoms is transferred to form a butene. An important aspect of the scheme is that the sulfur also functions as a nucleophile, carrying out C–S bond cleavage by hydrogen abstraction from the adsorbates. (Scheme 2). Thus, the NiPS phase is capable of carrying out multiple functions. The sudden remarkable increase in activity after the formation of the NiPS phase indicates that the NiPS phase is highly active, and this activity may be related to its multifunctional character.

4. Conclusions

Supported Ni_2P is an active catalyst for hydrodesulfurization (HDS) of petroleum feed stocks, and an investigation was carried out, to determine its structure under reaction conditions and clarify the mechanism of thiophene HDS. For this purpose, simultaneous time-resolved (STR) studies of a Ni_2P/MCM-41 catalyst were carried out using in situ quick X-ray absorption fine structure (XAFS) spectroscopy with a spectral acquisition time of 10 s and Fourier transformed infrared (FTIR) absorption spectroscopy, together with time-resolved product analysis. This STR study revealed that the Ni–S species observed by XAFS could be assigned to an active nickel phosphosulfide phase (NiPS). Time-resolved FTIR measured simultaneously indicated that adsorbed tetrahydrothiophene (THT) was a reaction intermediate. The STR study was proved to be a powerful tool for the precise study of reaction intermediates and the reaction path.

Acknowledgments

This work was supported by the US Department of Energy, Office of Basic Energy Sciences, through Grant DE-FG02-963414669, a JST Grant-in-Aid for Scientific Research (Category S, No. 16106010 and Category B, No. 16360405) and the Cooperative Research Program of Catalysis Research Center, Hokkaido University (Grant #10B1001, and #10B2009). The XAFS experiments were conducted under approval of PF-PAC (Project No. 2010G127, 2008G129, 2006G109). The authors thank Dr. Shinichi Nagamatsu at the University of Electro-Communications and Prof. Takashi Fujikawa at Chiba University for theoretical simulation of XANES to confirm our results. We also thank Mr. Shigeru Bando for creating an image of the cell in Fig. 1.

References

[1] W. Li, B. Dhandapani, S.T. Oyama, Chem. Lett. (1998) 207.
[2] S.T. Oyama, T. Gott, H. Zhao, Y.-K. Lee, Catal. Today 143 (2009) 94.
[3] A.W. Burns, A.F. Gaudette, M.E. Bussell, J. Catal. 260 (2008) 262.
[4] H. Topsoe, B.S. Clausen, F.E. Massoth, Hydrotreating Catalysis, Springer-Verlag, New York, 1996.
[5] S.T. Oyama, P. Clark, V.L.S. Teixeira da Silva, E.J. Lede, F.G. Requejo, J. Phys. Chem. B 105 (2001) 4961.
[6] P. Clark, W. Li, S.T. Oyama, J. Catal. 200 (2001) 140.
[7] S.T. Oyama, J. Catal. 216 (2003) 343.
[8] S.T. Oyama, X. Wang, Y.-K. Lee, K. Bando, F.G. Requejo, J. Catal. 210 (2002) 207.
[9] S.J. Sawhill, K.A. Layman, D.R. Van Wyk, M.H. Engelhard, C. Wang, M.E. Bussell, J. Catal. 231 (2005) 300.
[10] A. Wang, L. Ruan, Y. Teng, X. Li, M. Lu, J. Ren, Y. Wang, Y. Hu, J. Catal. 229 (2005) 314.
[11] S.T. Oyama, X. Wang, F. Requejo, T. Sato, Y. Yoshimura, J. Catal. 209 (2005) 1.
[12] Y. Shu, Y.-K. Lee, S.T. Oyama, J. Catal. 236 (2005) 112.
[13] S.T. Oyama, Y.-K. Lee, J. Catal. 258 (2008) 393.
[14] S.J. Sawhill, D.C. Phillips, M.E. Bussell, J. Catal. 215 (2003) 208.
[15] X. Duan, Y. Teng, A. Wang, V.M. Kogan, X. Li, Y. Wang, J. Catal. 261 (2009) 232.
[16] J. Hyung, X. Ma, C. Song, Y.-K. Lee, S.T. Oyama, Energy Fuels 19 (2005) 353.
[17] S.T. Oyama, T. Gott, K. Asakura, S. Takakusagi, K. Miyazaki, Y. Koike, K.K. Bando, J. Catal. 268 (2009) 209.
[18] K.K. Bando, T. Wada, T. Miyamoto, K. Miyazaki, S. Takakusagi, T. Gott, A. Yamaguchi, M. Nomura, S.T. Oyama, K. Asakura, J. Phys.: Conference Series 190 (2009) 012158.
[19] J.W. Couves, J.M. Thomas, D. Waller, R.H. Jones, A.J. Dent, G.E. Derbyshire, G.N. Greave, Nature 354 (1991) 465.
[20] B.S. Clausen, Catal. Today 39 (1998) 293.
[21] A.J. Dent, Topics Catal. 18 (2002) 27.
[22] J.G. Mesu, A.d.M.J. van der Eerden, F.M.F. de Groot, B.M. Weckhuysen, J. Phys. Chem. B 109 (2005) 4042.
[23] M.A. Newton, A.J. Dent, S.G. Fiddy, B. Jyoti, J. Evans, Catal. Today 126 (2007) 64.
[24] A.J. Dent, J. Evans, S.G. Fiddy, B. Jyoti, M.A. Newton, M. Tromp, Faraday Discuss. 138 (2008) 287.
[25] M.A. Newton, Topics Catal. 52 (2009) 1410.
[26] A. Kubacka, A. Martínez-Arias, M. Fernádez-García, M. Di Michiel, M.A. Newton, J. Catal. 270 (2010) 275.
[27] N.S. Marinkovic, Q. Wang, A.I. Frenkel, J. Synchrotron Rad. 18 (2011) 447.
[28] C.-F. Cheng, D.H. Park, J. Klinowski, J. Chem. Soc., Faraday Trans. 93 (1997) 193.
[29] S.T. Oyama, X. Wang, Y.-K. Lee, W.-J. Chun, J. Catal. 221 (2004) 263.
[30] V.T. da Silva, L.A. Sousa, R.M. Amorim, L. Andrini, S.J.A. Figueroa, F.G. Requejo, F.C. Vicentini, J. Catal. 279 (2011) 88.
[31] K.K. Bando, Y. Koike, T. Kawai, G. Tateno, S.T. Oyama, Y. Inada, M. Nomura, K. Asakura, J. Phy. Chem. C 115 (2011) 7466.
[32] T. Kawai, S. Sato, W.-J. Chun, K. Asakura, K.K. Bando, T. Matsui, Y. Yoshimura, T. Kubota, Y. Okamoto, Y.-K. Lee, S.T. Oyama, Phys. Scr. T115 (2005) 822.
[33] T. Kawai, S. Sato, S. Suzuki, W.-J. Chun, K. Asakura, K.K. Bando, T. Matsui, Y. Yoshimura, T. Kubota, Y. Okamoto, Y.-K. Lee, S.T. Oyama, Chem. Lett. 32 (10) (2003) 956.
[34] T. Kawai, K.K. Bando, Y.-K. Lee, S.T. Oyama, W.-J. Chun, K. Asakura, J. Catal. 241 (2006) 20.
[35] Personal communication with S. Nagamatsu, and T. Fujikawa.